OTPA method-based contribution analysis of components on the vibration of fuel cell in fuel cell vehicles

Zequn Nan[1]
Matthias Behrendt[2]
Mengting Lu[3]
Manuel Petersen[4]
Albert Albers[5]

IPEK – Institute of Product Engineering at Karlsruhe Institute of Technology (KIT)
Kaiserstraße 10
76131 Karlsruhe, Germany

ABSTRACT

Due to the introduction of auxiliary components in fuel cell vehicle powertrains and absence of internal combustion engine, the vibration sources and transfer paths are very different from conventional vehicles. These vibrations interact on the output performance of the fuel cell system. Therefore, it is necessary to investigate the vibration characteristics of the fuel cell system under vehicle operating conditions. The IPEK conducted vehicle measurements regarding different driving manoeuvres and environments. In order to quantitatively evaluate the contributions of each vibration source on the total vibration of fuel cell, frequency-domain contribution is investigated based on Operational Transfer Path Analysis method with the Singular Value Decomposition as well as Principal Component Analysis. The results of vibration in Z-direction in the vehicle coordinate system show that the H_2 pump dominantly contributes to the vibration of the fuel cell in a wide range of frequency in the majority of the driving manoeuvres. However, the results vary in various driving manoeuvres, environments and frequencies. The paper will discuss in detail the vibrational contributions in X-, Y- and Z-direction.

1. INTRODUCTION

Because of the advantages of higher energy efficiency, zero local pollution and zero local carbon emissions when comparing with Internal Combustion Engine (ICE), the hydrogen Fuel Cell (FC), an electrochemical reactor that consumes hydrogen and air and produces electricity, is gradually applied in mobility as alternative power source. Like other components, the FC system in a Fuel Cell Vehicle (FCV) operates in a vibrating environment. However, vibrations will lead to an influence on the performance of the FC such as output voltage and power [1-4]. And this influence will also vary with

[1] zequn.nan@partner kit.edu

[2] matthias.behrendt@kit.edu

[3] ufdmk@student.kit.edu

[4] manuel.petersen@kit.edu

[5] albert.albers@kit.edu

the change of vibration parameters e.g. frequency and amplitude [1]. Thus, the performance of the FC must be validated in vibrating environments in future development processes of FCs.

In the FC powertrain systems (see Figure 1), more components with moving parts such as, FC air compressor, H_2 pump etc. are newly introduced in vehicles. They distribute from front to the rear of in FCVs. As potential noise and vibration sources, components in FC powertrains have very different NVH behaviours and transfer paths from the ICE in conventional vehicles, which finally lead to novel NVH phenomena in FCVs. The vibrations experienced by FCs are mainly from on-board components and road roughness transferred by wheels and suspension. Therefore, considering the previous studies [1-4] and demand for validation of FCs in vibrating environments, it is necessary to investigate the vibrations experienced by the FC stack under common driving manoeuvres and environments (road surfaces).

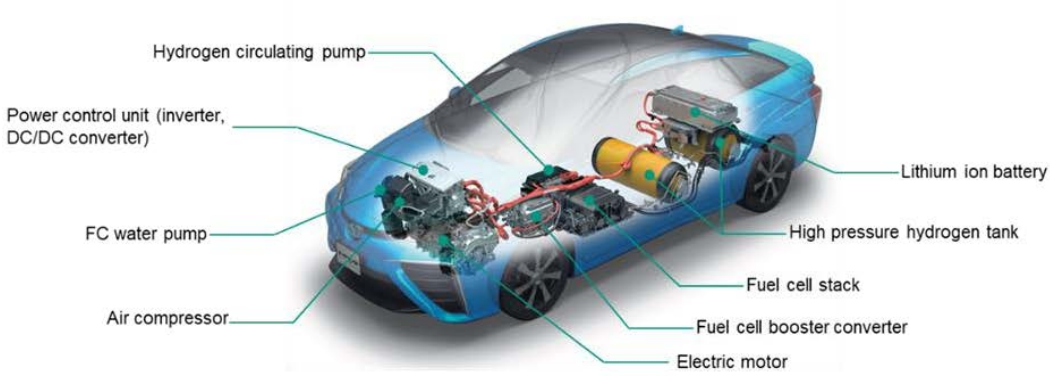

Figure 1: FC powertrain system in Toyota Mirai [5]

Based on the previous work [6] of IPEK – Institute of Product Engineering at Karlsruhe Institute of Technology (KIT), this work quantitatively evaluates contributions of each vibration source on the total vibration of the FC. Operational Transfer Path Analysis (OTPA) method is applied by conducting vehicle measurements with Toyota Mirai in context of the IPEK-X-in-the-Loop-Framework regarding different driving manoeuvres and environments. Considering crosstalk of raw data, Singular Value Decomposition (SVD) and Principal Component Analysis (PCA) are also used to eliminate path misjudgement and improve the accuracy of the contribution evaluation.

2. METHOD

2.1. OTPA method

OTPA is a fast and efficient method to identify critical vibration transfer paths and source contributions in vehicle development process [7]. Based on the multi-input and multi-output transmissibility calculation principle, OTPA method uses the transfer function matrix between a set of operational passive side responses and target responses to represent the paths of the vibration as shown in Equation 1 [8]:

$$\begin{bmatrix} Y_1^{(1)} & Y_2^{(1)} & \dots & Y_k^{(1)} \\ Y_1^{(2)} & Y_2^{(2)} & \dots & Y_k^{(2)} \\ \dots & \dots & \dots & \dots \\ Y_1^{(m)} & Y_2^{(m)} & \dots & Y_k^{(m)} \end{bmatrix} = \begin{bmatrix} T_{11} & T_{12} & \dots & T_{1k} \\ T_{21} & T_{22} & \dots & T_{2k} \\ \dots & \dots & \dots & \dots \\ T_{n1} & T_{n2} & \dots & T_{nk} \end{bmatrix} \begin{bmatrix} X_1^{(1)} & X_2^{(1)} & \dots & X_n^{(1)} \\ X_1^{(2)} & X_2^{(2)} & \dots & X_n^{(2)} \\ \dots & \dots & \dots & \dots \\ X_1^{(m)} & X_2^{(m)} & \dots & X_n^{(m)} \end{bmatrix} \quad (1)$$

where $Y_j^{(p)}$ is the target response, the output of path *j (j≤k)* in measurement *p (p≤m)*, $X_j^{(p)}$ is the passive side response of the source, the output of path *j (j≤k)* in measurement *p (p≤m)*, T_{nk} is the transmissibility function matrix.

The transfer function of OTPA method is based on the response-response transmissibility matrix calculation, which is different from conventional Transfer Path Analysis (TPA) method based on the

frequency response function. The OTPA method thus significantly reduces the measuring and modelling time comparing to TPA method by requiring only operational measurements of the passive side responses measured at the load and target locations [9]. Therefore, this method is widely applied in the vehicle development for its rapidity and simplicity to identify the main excitation source and transfer path.

After acquiring the data by vehicle operational measurements, the output matrix and input matrix in Equation 1 can be determined. The transmissibility functions can then be calculated with the inverse matrix, as seen in Equation 2:

$$T = G_{xx}^{-1} G_{xy} = (X^T X)^{-1} (X^T Y) \tag{2}$$

where G_{xx} is the auto power spectrum matrix, G_{xy} is the cross power spectrum matrix, X is the sources input matrix, Y is the targets output matrix.

2.2. SVD- and PCA-based OTPA method

The traditional OTPA method presents errors in contribution calculation and misjudgements in the transfer function determination because of data noise and crosstalk. Therefore, it is significant to improve the accuracy of OTPA method by using SVD and PCA [10].

2.2.1 Singular Value Decomposition

SVD is used to reduce the influence of noise on data evaluation by iteratively finding and eliminating the strongest correlation between components of a data set, till the full data set is defined. This can be realized by running the remaining data set through SVD and making each value orthogonal to other singular values. Equation 3, the mathematical expression of SVD is:

$$X = U \Sigma V^T \tag{3}$$

where X is the sources input matrix, U is the unitary column-orthogonal matrix, Σ is the singular value matrix and V^T is the transpose of an unitary column-orthogonal matrix V.

The result of SVD can be directly used to compute the transmissibility functions matrix T, as shown in Equation 4:

$$T = V \Sigma^{-1} U^T Y \tag{4}$$

where V is the unitary column-orthogonal matrix, Σ^{-1} is the invers of a singular value matrix Σ, U^T is the transpose of an unitary column-orthogonal matrix U, Y is the targets output matrix.

2.2.2 Principal Component Analysis

PCA is applied to decrease the influence of unnecessary frequency components by reducing a data set that consists of a large number of interrelated variables to a smaller data set that preserves most of the original information [11]. Specifically, PCA is an orthogonal transformation to remove correlation between data sets and thus reduce the crosstalk. The variables obtained after the orthogonal transformation are called Principal Components (PC), which are ranked according to their variances within the data set.

The PC scores are obtained by Equation 5:

$$Z = U \Sigma \tag{5}$$

where Z is the PC scores matrix, U is the unitary column-orthogonal matrix, Σ is the singular value matrix.

The contribution of each PC to the overall signal can be evaluated by dividing Z by the total sum of the PC scores, which yields a percentage contribution for each PC score. For each analysis, a threshold under which the components will be discarded is determined, thereby eliminating crosstalk.

2.3. Contribution calculation

After building up the transfer model between response of sources and targets and validating its accuracy, contribution calculation, also known as response synthesis, can be carried out in the frequency domain by Equation 6:

$$Y_{s_j}^{(p)} = X^{T}{}_{j}^{(p)} \cdot T_j \tag{6}$$

where $Y_{s_j}^{(p)}$ is the contribution matrix of path j in measurement p, $X^{T}{}_{j}^{(p)}$ is the transpose of sources input matrix of path j in measurement p, T_j is the transmissibility function of path j.

The response of target can thus be decomposed and the contribution of each path or source can be quantified in the frequency domain.

3. MEASUREMENT SETUP IN CONTEXT OF THE IPEK-XIL-FRAMEWORK

3.1. The IPEK-X-in-the-Loop-Framework

The IPEK-X-in-the-Loop-Framework (see Figure 2) is a holistic and integrated framework for development and validation to meet the challenges of increasing complexity of modern vehicle concepts [12]. It integrates simulation and test on each level of validation, and considers the three interacting systems driver, vehicle and environment. The "X" represents the System in Development (SiD), which can either be a virtual model, physical or mixed virtual-physical object in different layers in this framework, the element-, the subsystem-, the system- and the vehicle-in-the-loop. The validation of the SiD can be conducted in each layer in the context of the system driver and environment by using realistic or generic manoeuvres and test cases [13]. Therefore, it is possible to do the closed-loop test in each layer considering the effect of the driver behaviour and the environment.

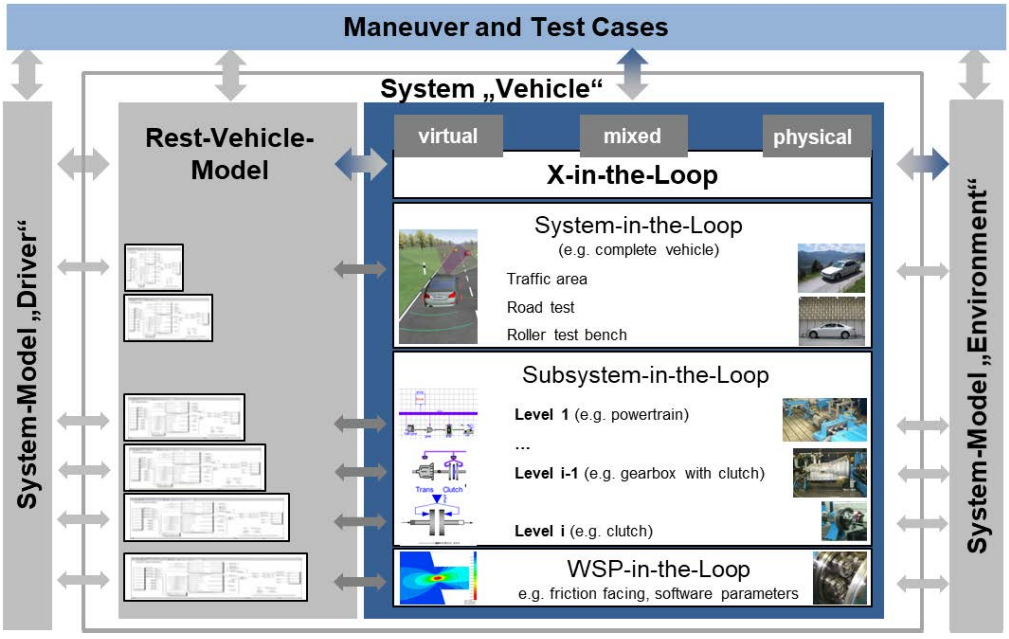

Figure 2: The IPEK-X-in-the-Loop-Framework [12]

The measurement in this paper is also performed in context of the IPEK-X-in-the-Loop-Framework. The SiD, an FCV hereby, was measured in the layer of vehicle-in-the-loop under various environments (road surfaces) and with different driving manoeuvres driven by a real driver and a driving robot.

3.2. Test Environments and Manoeuvres

Similar to the measurement in the previous work of IPEK [6], the vehicle is tested in three environments with different pavements, street with paved road, sett pavement and acoustic roller test bench.

Street with paved roads are the most generic scenario in vehicle operating. They provide a very wide speed range and low roughness for vehicles. The performance of vehicles can thus be well revealed when driving on them. Sett pavements, which are paved with rectangular quarried stone,

were designed to provide more grip to horse hooves before. They are still kept in many European and American cities and towns today. The excitation caused by the unevenness of sett pavements can be strongly transferred to the on-board components and passengers. The speed limit on sett pavements is usually not higher than 50 km/h. The IPEK acoustic roller test bench with Vehicle-in-the-Loop-Technology [14] in a semi-anechoic chamber (see Figure 3 left) can reproduce normal driving on the street. The tested FCV is fixed by hooks in a two-point (front and rear) fixation. Considering the error and difference caused by a real driver in different tests of same driving manoeuvre, the driving robot (see Figure 3 right) replaced the real driver during the measurement on the roller test bench.

Figure 3: Acoustic roller test bench (left) and driving robot SAP 2000 (right)

The driving manoeuvres in this work contains most common scenarios such as constant speed driving and accelerating. Additionally, the air conditioner (A/C) status and vehicle driving modes are considered as well. When the tested vehicle is driving, an obvious and stable roaring noise can be clearly heard after turning on the A/C switch. It is superimposed on the existing vehicle noise. It is almost certain that the roaring noise comes from the A/C compressor operating. It can also be assumed that the vibration generated by the A/C compressor is transmitted to the FC. The tested FCV provides 3 driving modes, normal, eco and power. The components in the FC powertrain behave differently in the various driving modes.

The driving manoeuvres, conducted in this work, are listed in Table 1. The vibration behaviours of components and the FC in these manoeuvres and driving modes are various. This ensures the adequacy and diversity of data for further calculation.

Table 1: Driving manoeuvres in measurements of the tested FCV

Vehicle status		**Driving manoeuvres when test on…**		
A/C status	Driving modes	Paved road	Sett pavement	Acoustic roller test bench
On	Normal	30, 40, …, 110, 120 km/h	7 (creep), 30, 40 km/h	7 (creep), 30, 40, …, 110, 120 km/h
	Eco			
	Power			
Off	Normal			
	Eco			
	Power			

3.3. Accelerometers Positioning

Triaxial accelerometers are mounted on surfaces of components to acquire acceleration data. Components with rotary parts (e.g. compressor, pump, motor) and moving parts (e.g. valve, wheel mounting), which are regarded as potential vibration sources, and the FC stack are investigated in this work. Table 2 show the positioning of the accelerometers and the corresponding positions are marked in Figure 4.

Table 2: Positioning of the accelerometers in the tested vehicle

Accelerometers Positions		
FC air compressor (A1)	A/C compressor (A2)	E-motor (A3)
H_2 pump (A4)	FC stack (A5)	Hydrogen supply regulator (A6)
Front hydrogen tank valve (A7)	Rear hydrogen tank valve (A8)	Left front wheel mounting (A9)
Right front wheel mounting (A10)	Left rear wheel mounting (A11)	Right rear wheel mounting (A12)
Motor inverter cooling water pump (A13)	Inverter cooling water pump (A14)	FC cooling water pump (A15)

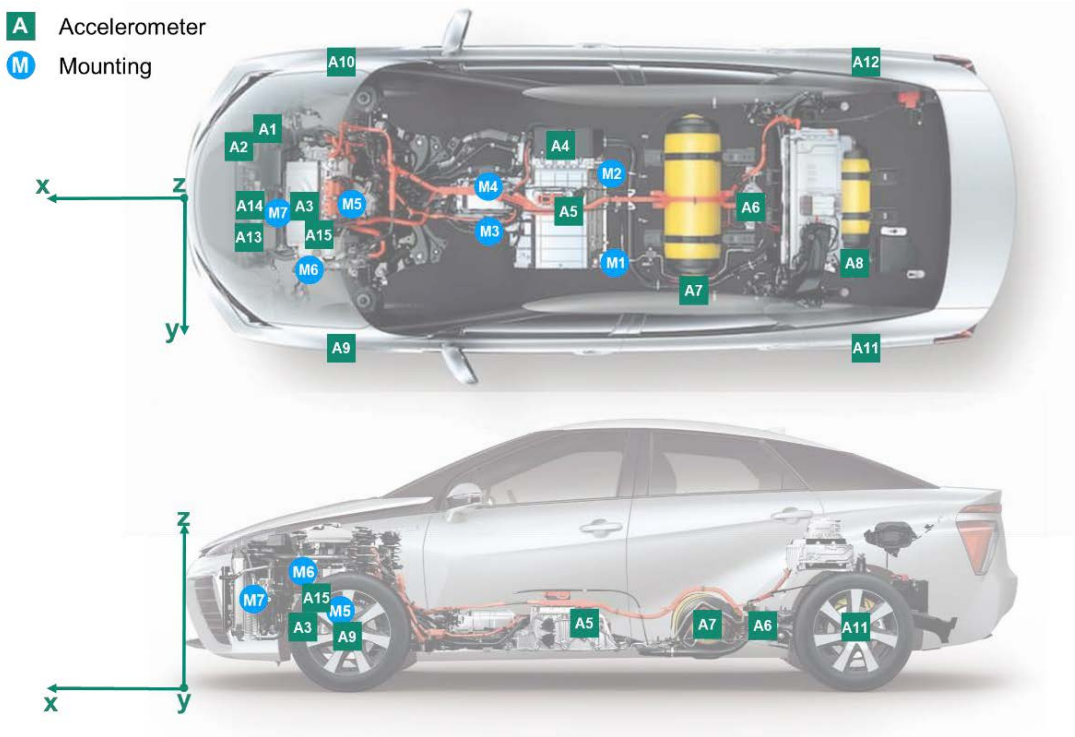

Figure 4: Positioning of the accelerometers in the test vehicle

4. RESULTS AND ANALYSIS

By following the knowledge in section 2, the data acquired from the measurements was used to calculate the total contribution from sources on the FC in specific manoeuvres and decomposition of each path (sources) at the frequencies interest. The contributions of each source were then be quantitatively evaluated. The results are presented in order of vibration direction in the Z-, X- and Y-direction of the vehicle coordinate system.

4.1. Result of vibration in Z-direction

4.1.1 Results at different speeds

Due to very little difference of roughness between paved road and roller test bench, the results show similarity when the vehicle is tested in these two environments. The following presented results focus more on the measurements on the roller test bench with the driving robot. Figure 5 shows the total contribution on the FC at speed of 40 to 120 km/h. High contribution values occurs in frequency ranges below 50 Hz and 480-500 Hz. The result of frequency below 50 Hz has more representativeness in the measurement on sett pavements, so it will be discussed later.

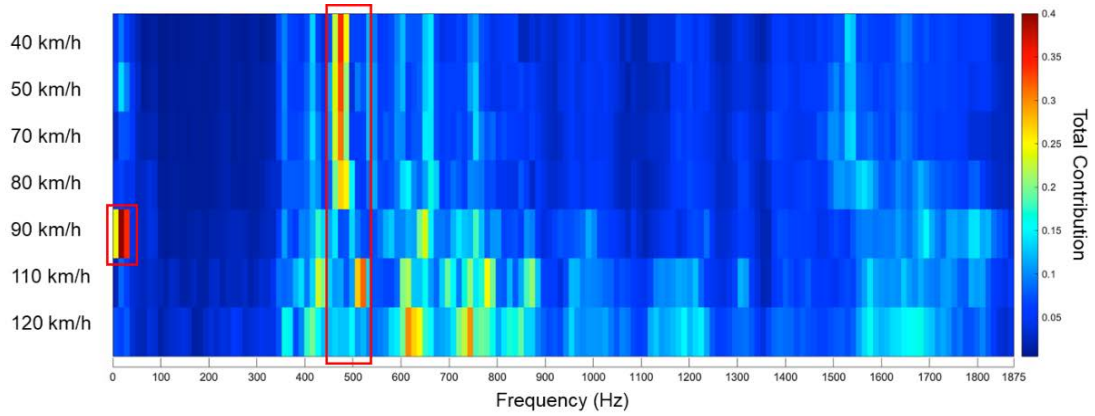

Figure 5: Total contribution on the FC in Z-direction from 40, 50, 70, 80, 90, 110 and 120 km/h on the roller test bench

Figure 6 shows and compares the contribution of sources at different speeds at around 480 Hz. The H_2 pump and the valve of hydrogen tank valve have the first and second largest contributions on the vibration of the FC at 40 and 80 km/h. However, as the speed increases, their contributions will decrease and increase respectively and swap places in the maximum contribution ranking as shown in Figure 6 (right). The e-motor, which is expected to have the strongest vibration, has a negative contribution on the vertical vibration of the FC, and the higher the vehicle speed the larger its negative contribution is. In addition, the negativity of contribution from the inverter cooling water pump should not be ignored.

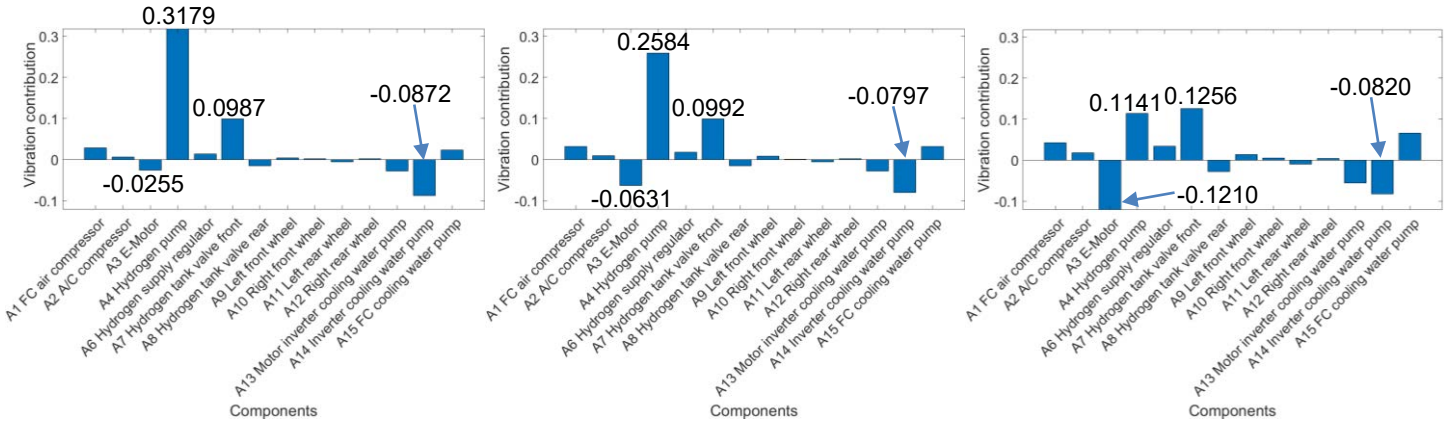

Figure 6: Contribution of sources on the FC in Z-direction at ca. 480 Hz on the roller test bench. Total contribution at 40 km/h: 0.3372 (left); total contribution at 80 km/h: 0.2692 (middle); total contribution at 120 km/h: 0.1261 (right)

4.1.2 Results on different pavements

When comparing the total contribution on the FC tested on different pavements (see Figure 7), a significant increasing below 100 Hz can be clearly observed when the pavement is rougher. Moreover, a relatively large total contribution appears again around 480 Hz with similarly large contribution values (0.3372 on the roller test bench, 0.3301 on the paved road and 0.3101 on the sett pavement). The results of contribution decomposition around 480 Hz have hardly any difference between three pavements and are almost identical to the Figure 6 (left). Therefore, there is no redundant descriptions here.

By comparing the results of contribution decomposition around 30 Hz at the three pavements in Figure 8, it is found that the contributions from the left wheels are positive while from the right wheels are negative as marked with red rectangle. Their absolute value increases as the unevenness of the pavements rises. Among all 14 investigated sources, the H_2 pump dominantly contributes on the FC around 30 Hz and its contribution is much larger than the contribution of the wheels, which was not expected.

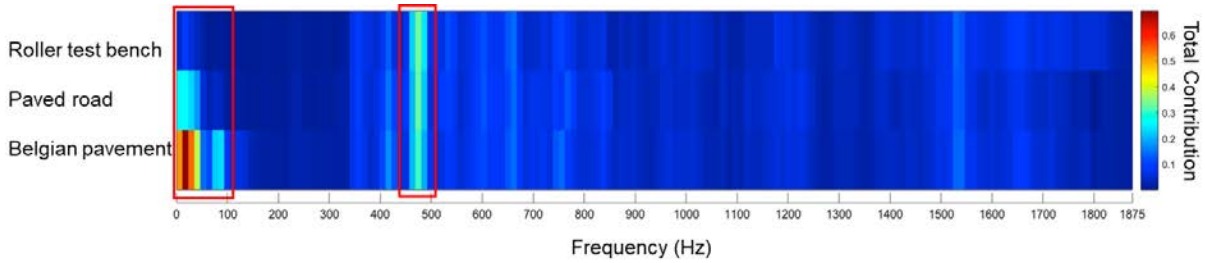

Figure 7: Total contribution on the FC in Z-direction on different pavements at 40 km/h

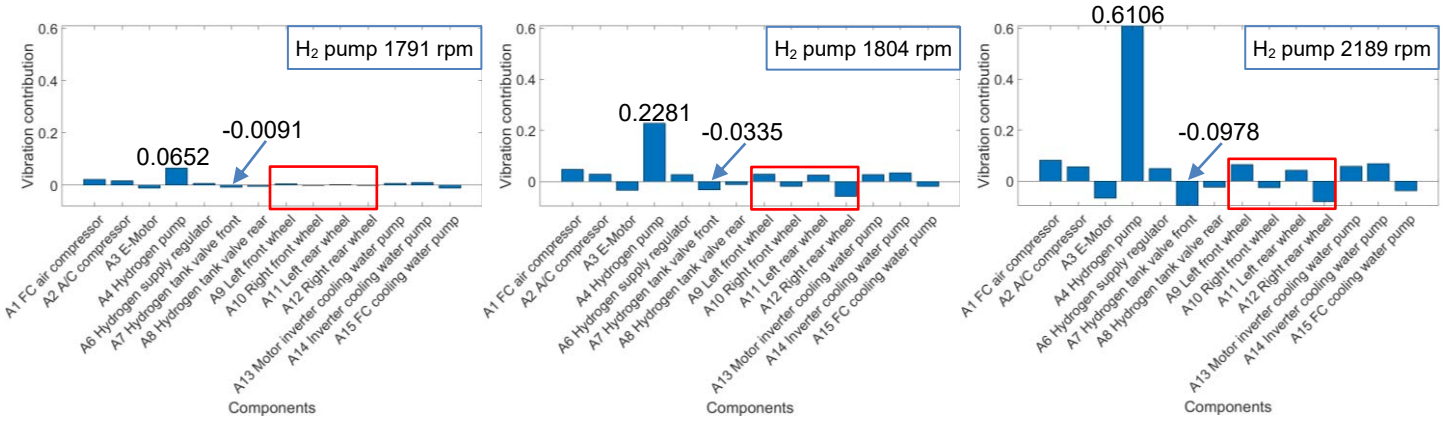

Figure 8: Contribution of the sources on the FC in Z-direction at ca. 30 Hz at 40 km/h. Roller test bench total contribution: 0.0922 (left); paved road total contribution: 0.2656 (middle); sett pavement: total contribution 0.6929 (right)

It is inferred that there are two reasons. On the one hand, the frequency corresponding to the rotating speed of the H_2 pump is between 20 and 40 Hz. This implies that the first order resonance is probable to appear in this range. On the other hand, the connection between the H_2 pump and the FC has a high rigidity, because they are adjacent and there is no visible damper or absorber between them [6]. This results in them being exposed together to vibrations transmitted from other sources, with very similar vibration responses. This can also explain why the H_2 pump has the largest contribution at the frequency where the total contribution on the FC is relatively large.

Furthermore, driving on rougher road requires a higher power of the vehicle. For the FC powertrain systems, a higher H_2 supply is needed in this situation, so the rotating speed of the H_2 pump rises and the vibration is stronger. Accordingly, its contribution increases with more unevenness.

4.2. Result of vibration in X-direction

As for the result of vibration in X-direction (see Figure 9), the frequency range with the largest contribution is between 1500 and 1550 Hz. A further contribution result around 1535 Hz is shown in Figure 10.

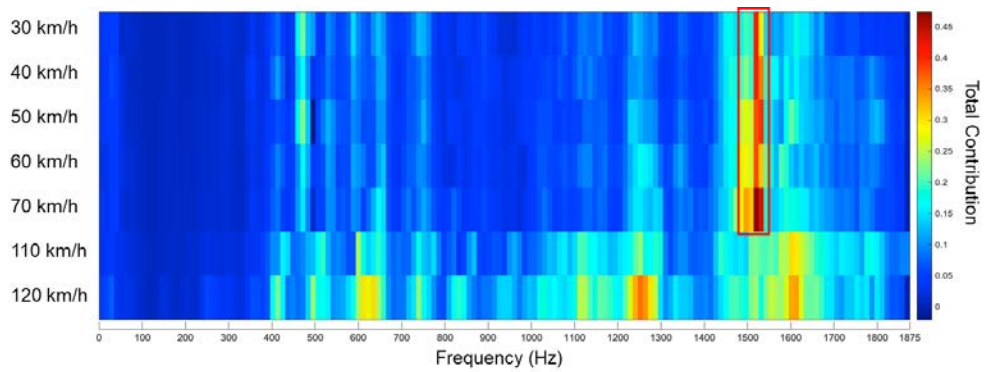

Figure 9: Total contribution on the FC in X-direction from 30 to 70, 110 and 120 km/h on the roller test bench

For the previously mentioned reasons, contribution from the H_2 pump on vibration of FC remains the largest. It is also notable, that the FC air compressor, the inverter cooling water pump and the FC cooling water pump have positive contributions, while the hydrogen supply regulator, the rear hydrogen tank valve and the left front wheel have negative contributions. The absolute values of their contributions become larger as the vehicle speed increases.

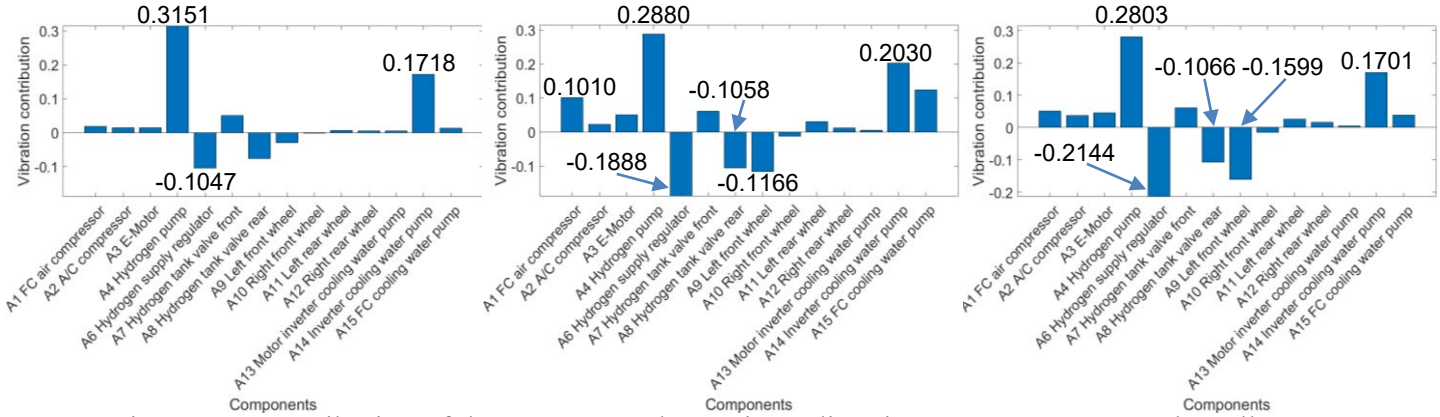

Figure 10: Contribution of the sources on the FC in X-direction at ca. 1530 Hz on the roller test bench. Total contribution at 40 km/h: 0.4025 (left); total contribution at 70 km/h: 0.4740 (middle); total contribution at 120 km/h: 0.2345 (right)

4.3. Result of vibration in Y-direction

The result of total contribution on the FC in Y-direction (see Figure 11) significantly differs from the results in Z- and X-direction. The largest total contribution in Y-direction is 0.2315 at around 30 Hz at speed of 90 km/h, while in Z-direction the largest is 0.5815 at around 30 Hz at speed of 90 km/h (Figure 5) and in X-direction the largest is 0.4740 at around 1530 Hz at speed of 70 km/h (Figure 9). This indicates that the FC has the lowest vibration in the horizontal direction. Another frequency range with large total contribution is between 700 and 800 Hz. The frequencies corresponding to these two red boxes are analysed in the following.

Besides the H_2 pump, the two rear wheels and motor inverter cooling water pump contribute greatly to the vibration of the FC around 30 Hz when the vehicle is driving at 90 km/h as seen in Figure 12 (left). However, at the frequency of 780 Hz (see Figure 12 (right)), top contributors are the FC air compressor, the H_2 pump and the e-motor. The contribution from the FC air compressor is even higher than the H_2 pump. The A/C compressor and the two front wheels contribute negatively on the vibration of the FC in Y-direction.

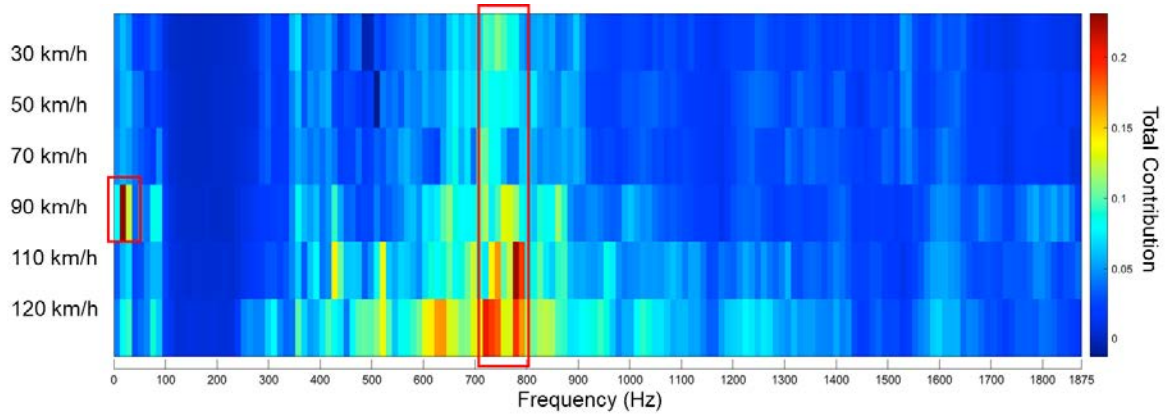

Figure 11: Total contribution on the FC in Y-direction at 30, 50, 70, 90, 110 and 120 km/h on the roller test bench

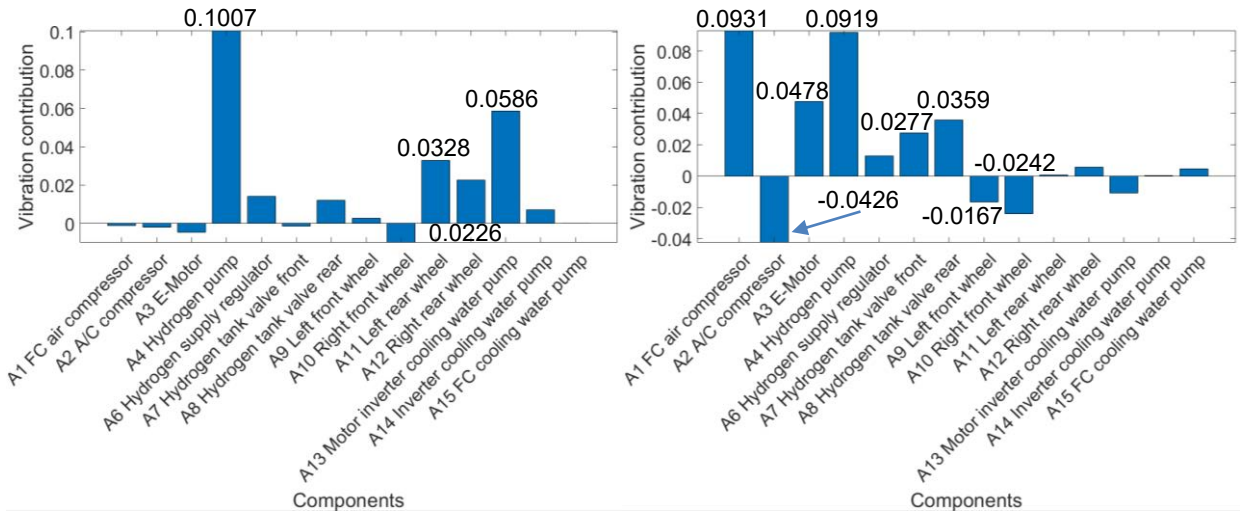

Figure 12: Contribution of the sources on the FC in Y-direction on the roller test bench. 90 km/h at ca. 30 Hz total contribution: 0.2315 (left); 110 km/h at ca. 780 Hz total contribution: 0.2265 (right)

5. CONCLUSIONS

FCs are more gradually used in e-mobility as alternative power source because of its advantages in efficiency and local emissions. A number of researches have shown that the performance of FCs can be affected by vibration. The FCs used in vehicles are exposed to vibration during the operating of FCVs. There is an obvious difference in the on-board vibrating environment between FCVs and traditional ICE vehicles due to different components and their layouts in the powertrain system. It is therefore necessary to investigate NVH issues in FCVs, particularly with regard to the vibrations experienced by FCs.

In this paper, the contribution from FCV's potential vibration sources on the total FC vibration was quantitatively evaluated in the frequency domain. Measurements with an FCV were firstly conducted in context of the IPEK-X-in-the-Loop-Framework in consideration of driver, driving manoeuvres and environments. Then, the SVD- and PVA-based OTPA method was applied to calculate the total contributions (response) on the FC (target) in the frequency domain and its decomposition of each component (sources) at frequencies with considerable contribution.

The results show that, the vibration of FC has the maximum total contribution in Z-direction of the vehicle coordinate system and the minimum in Y-direction. In most driving manoeuvres, the H_2 pump makes dominant contribution to the vibration of the FC over a wide range of frequency due to the highly rigid connection between them. The results vary in the different driving manoeuvres, pavements and frequencies. For instance, the vibration in Z-direction, when driving on the roller test bench at 40 and 80 km/h, the H_2 pump and the front hydrogen tank valve have the first and second largest contributions on the vibration of FC around 480 Hz. On the contrary, the e-motor and the inverter cooling water pump contribute negatively meanwhile. Results of measurements on different pavements indicate that the rougher the road, the greater the total contribution on the FC and the absolute value of wheel's contribution below 100 Hz. Large total contribution on the FC also appears around 1535 Hz in X-direction and around 30 and 780 Hz in Y-direction. At the frequency of 1535 Hz in X-direction, H_2 pump, FC air compressor, inverter cooling water pump and FC cooling water pump have significant positive contributions, while hydrogen supply regulator, rear hydrogen tank valve and left front wheel are negative contributors. As for Y-direction, H_2 pump, rear wheels and motor inverter cooling water pump contribute apparently around 30 Hz. FC air compressor, H_2 pump and e-motor have positive contributions at 780 Hz, but A/C compressor and front wheels have negative contributions.

However, it should be noted that, the results differ when the layout of FC powertrain system changes, which means a different transfer function. Therefore, similar investigations could be necessary for different FCVs.

6. ACKNOWLEDGEMENTS

This paper presents excerpts of work in the project „Methoden zur arbeitsteiligen, räumlich verteilten Entwicklung von H2-Brennstoffzellen-Fahrzeugen in Kooperation mit China - MorEH2“. The authors are grateful to the German Federal Ministry of Education and Research funding this project (Funding No.: 16EMO0316).

7. REFERENCES

1. Breziner, L., Peter, S., & Parsaoran, H. Effect of Vibration on the Polarization Curves of Polymer Electrolyte Membrane Fuel Cells. (2009).
2. Hou, Y., et al. An investigation of characteristic parameter variations of the polarization curve of a proton exchange membrane fuel cell stack under strengthened road vibrating conditions. *International journal of hydrogen energy*, **37.16 (2012)**, 11887-11893.
3. Santamaria, A. D., et al. Liquid water interactions with PEFC gas-diffusion layers: the effect of vibration. *ASME International Mechanical Engineering Congress and Exposition,* **Vol. 57441**. American Society of Mechanical Engineers, 2015.
4. Hou, Y., et al. Effect of strengthened road vibration on performance degradation of PEM fuel cell stack. *International Journal of Hydrogen Energy* **41.9 (2016)**: 5123-5134.
5. Toyota Europe. “Outline of the Mirai,” *https:// www.toyota- europe.com/download/cms/euen/Toyota%20Mirai%20FCV_Posters_LR_tcm-11 -564265.pdf*, 2019.
6. Nan, Z., Behrendt, M., Petersen, M., & Albers, A. NVH analysis of fuel cell with consideration of driving manoeuvres in FCV. *INTER-NOISE and NOISE-CON Congress and Conference Proceedings. Vol. 261. No. 2*. Institute of Noise Control Engineering, 2020.
7. De Klerk, Dennis, et al. Application of operational transfer path analysis on a classic car. *Proc. DAGA*. 2009.
8. Zhou, L. Transfer path analysis and control of floor vibration based on OTPA method. *Southwest Jiaotong University,* 2018.
9. Wu, Y. X., Zhou, H., & Wang, E. B. Comparison of classical and operational transfer path analysis in vehicle NVH improvement. *Advanced Materials Research.* **Vol. 396**. Trans Tech Publications Ltd, 2012.
10. Cheng, W., Blamaud, D., Chu, Y., Meng, L., Lu, J., & Basit, W. A. Transfer Path Analysis and Contribution Evaluation Using SVD-and PCA-Based Operational Transfer Path Analysis. *Shock and Vibration* **2020** (2020).
11. Toome, M. Operational transfer path analysis: A study of source contribution predictions at low frequency. *Chalmers University of Technology, Goteborg, Sweden* (2012).
12. Albers, A., & Düser, T. Implementation of a vehicle-in-the-loop development and validation platform. *FISITA World automotive congress.* **Vol. 2010**. (2010).
13. Albers, A., Behrendt, M., Fischer, J., & Lieske, D. Identification and definition of acoustic relevant limit values for electric vehicles. *14. Internationales Stuttgarter Symposium.* Springer Vieweg, Wiesbaden, 2014.
14. Institut of Product Engineering, Karlsruhe Institute of Technology. “ARP Acoustic Roller Test Bench with Vehicle-in-the-Loop Technology,” *https://www.ipek.kit.edu/downloads/ARP_Flyer_EN_ 140905.pdf*, 2014.